Coherence of polaronic transport in layered metals

2004 J. Phys.: Condens. Matter 16 6695

(http://iopscience.iop.org/0953-8984/16/37/006)

INSTITUTE OF PHYSICS PUBLISHING JOURNAL OF PHYSICS: CONDENSED MATTER

J. Phys.: Condens. Matter **16** (2004) 6695–6712 PII: S0953-8984(04)81223-2

Coherence of polaronic transport in layered metals

Urban Lundin[1] **and Ross H McKenzie**

Department of Physics, University of Queensland, Brisbane Qld 4072, Australia

E-mail: lundin@physics.uq.edu.au

Received 25 May 2004, in final form 30 July 2004
Published 3 September 2004
Online at stacks.iop.org/JPhysCM/16/6695
doi:10.1088/0953-8984/16/37/006

Abstract

Layered systems show anisotropic transport properties. The interlayer conductivity shows a general temperature dependence for a wide class of materials. This can be understood if conduction occurs in two different channels activated at different temperatures. We show that the characteristic temperature dependence can be explained using a polaron model for the transport. The results show an intuitive interpretation in terms of coherent and incoherent quasi-particles within the layers. Further, we extract results for the magnetoresistance, thermopower, spectral function and optical conductivity for the model and discuss application to experiments.

(Some figures in this article are in colour only in the electronic version)

1. Introduction

Layered materials show a range of interesting behaviour, ranging from high temperature superconductivity to giant and colossal magnetoresistance. A common feature of some of these materials (see for example [1–3]) is that they show a peak in the interlayer resistivity as a function of temperature. In some cases there is also a peak in the intralayer resistivity. We can identify different temperature scales, from experiment. $T_{\perp}^{\max}$ determines the maxima in the interlayer resistivity. $T_{\parallel}^{\max}$ determines the maxima in the intralayer resistivity. Besides this, recent angle resolved photoemission (ARPES) experiments [4] concluded that the peak in the interlayer resistivity is closely related to intralayer coherence, and that there is a crossover for the spectral function from being coherent to being incoherent at a temperature T^{coh}. This idea that the scattering within the layers affects the transport between the layers has recently been investigated by Vozmediano *et al* [5]. All of this can be explained if there are two mechanisms of transport [6, 9]. One, a coherent mechanism, dominates at low temperatures, while at elevated temperatures an incoherent contribution starts to dominate. In this paper we will demonstrate that polaronic transport can be the mechanism providing this physics. This

[1] Author to whom any correspondence should be addressed.

Table 1. Temperature scales in experiment for different materials. n.s. means that the peak is not seen in the experiment, indicating that, if it is there, it is higher than the temperature range scanned in the experiment, n.a. means that the result is not available to our knowledge.

Material	$T_{\perp}^{\max}$ (K)	$T_{\parallel}^{\max}$ (K)	T^{coh} (K)
$(Bi_{0.5}Pb_{0.5})_2Ba_3Cu_2O_y$ [4]	200	n.s.	∼180
$NaCo_2O_4$ [4]	180	n.s.	∼150
$La_{1.4}Sr_{1.6}Mn_2O_7$ [1]	100	270	n.a.
Sr_2RuO_4 [2]	130	n.s.	n.a.
$TmBa_2Cu_3O_{6.41}$ [6]	127	n.s.	n.a.
$(TMTSF)_2PF_6$ [7]	90	n.s.	n.a.
κ-(BEDT-TTF)$_2$Cu(SCN)$_2$ [8]	95	100	n.a.

gives an intuitive explanation for the different temperature scales associated with transport and coherence. We extend the idea presented by Alexandrov and Bratkovsky [10], and apply it to *layered* transport. In that paper they discussed (bi)polaron formation within giant magnetoresistance materials.

Another powerful tool when studying polaronic transport is the thermopower. At high temperatures the conductivity is activated and the resistivity shows an exponential temperature dependence with a gap E_σ; the thermopower usually shows a $1/T$ behaviour where the barrier is E_{s}. One signature of polaronic transport is that $E_{\mathrm{s}} \ll E_\sigma$, whereas for normal semiconductors (where the transport is activated) we have $E_{\mathrm{s}} = E_\sigma$ [11]. From comparing the high temperature electrical resistivity and thermopower, a number of experimentalists have argued for the existence of small polarons in $LaMnO_3$ compounds [12–14]. Further evidence for small polarons can be found in neutron scattering data, where the polaron induces a local deformation of the lattice [15–17]. Measurements of thermopower in different directions in an organic quasi-two-dimensional crystal found differences in behaviour between the interlayer thermopower and the interlayer one [18]. Further, the presence of polarons was confirmed by photoemission experiments [19].

The approach that we present is based on known approximations for the polarons [20, 21]. Recent dynamical mean field (DMFT) calculations made on the transport of small polarons [22] indicate that the approximations that we are going to use overestimate the resistivity, and the exact functional behaviour of the resistivity. The results of Fratini *et al* [22] show that there are two temperature regions. One is a semiconducting region where transport is heavily influenced by phonon fluctuations. Then there is a non-adiabatic regime, which compares mostly to the small polaron regime in the Holstein model. Here, however, we are more concerned with transitions between different regions of small polaron transport, not so much with the exact details, and it seems that the approximations that we use do capture the essential physics. We do not claim that polarons are responsible for all the observed effects, simply that they can provide some insight into the physics of layered systems. For instance, for the manganites it seems that the double-exchange model is the preferred one (see [23] and references therein), although another explanation, in terms of a carrier density collapse due to bipolarons and their magnetic features [24], is gaining interest. Even the thermopower seems to be consistent with this model [25]. There are also theories using a combination of double-exchange models and polarons for the localized structure [26]. A shorter presentation of some of the results from this paper has been previously published [27]. We have also investigated the problem of angular magnetoresistance oscillations in layered metals arising from incoherence [28].

The layout of the paper is as follows. In section 2 we present the model, and the small polarons are introduced in section 3 with the decay and Green function. In section 4 we turn

to the transport properties for the intralayer and interlayer currents and thermopower. We conclude with a calculation of the optical properties, section 4.4, and a special case of the magnetoresistance, section 4.5.

2. Model Hamiltonian

We start with a Holstein model [29] for an infinite system where the electrons interact with bosons. The Hamiltonian is

$$\mathcal{H} = \sum_i \epsilon^0 c_i^\dagger c_i + \sum_{\mathbf{q}} \hbar\omega_{\mathbf{q}} a_{\mathbf{q}}^\dagger a_{\mathbf{q}} + \sum_{\langle i\eta\rangle} t_{i\eta} c_\eta^\dagger c_i + \sum_{i,\mathbf{q}} M_{\mathbf{q}} c_i^\dagger c_i \mathrm{e}^{\mathrm{i}\mathbf{q}\cdot\mathbf{R}_i}(a_{\mathbf{q}} + a_{-\mathbf{q}}^\dagger), \tag{1}$$

where ϵ^0 is the on-site energy, $\omega_{\mathbf{q}}$ is the dispersion of the bosons, $t_{i\eta}$ is the integral of hopping between neighbouring sites i and η, $M_{\mathbf{q}}$ is the coupling between the bosons and the electrons. We want to emphasize that we will talk about bosons, since the theory will look the same for all types of boson with a coupling given in the Hamiltonian above. The bosons can be phonons, spin waves, plasmons or any other type fulfilling bosonic commutation rules. Since we want to study layered systems we split the hopping into that parallel and perpendicular to the layers, $t_\parallel$ and $t_\perp$ respectively, where $t_\parallel \gg t_\perp$. We only include hopping between nearest neighbours, both for the intralayer and the interlayer hopping. This enables us to write the Hamiltonian in a way more adapted to the layered case, shown in figure 1. The nature of the transport depends on how $t_\parallel$ and $t_\perp$ compare with Γ, the scattering rate due to the bosons. We assume that $\Gamma > t_\perp$, so that the interlayer transport can be described by considering two decoupled layers—meaning that the electrons scatters many times within the layers before jumping to the next [5, 2, 27, 28]. We assume that we can decouple the bosons within each layer separately, i.e., the bosons are localized in each layer; the only interaction between bosons in different layers comes from the electron tunnelling, but this occurs more seldom than the electron scattering of bosons in each layer. The Hamiltonian can be specified for this system. Two layers are coupled with a hopping Hamiltonian. Within each layer the electrons can hop but there is a coupling to a bosonic degree of freedom in each layer. We then use the Hamiltonian

$$\mathcal{H} = \mathcal{H}_1 + \mathcal{H}_2 + \mathcal{H}_t \tag{2}$$

where

$$\mathcal{H}_1 = \sum_i \epsilon^0 c_i^\dagger c_i + \sum_{\mathbf{q}} \hbar\omega_{\mathbf{q}} a_{\mathbf{q}}^\dagger a_{\mathbf{q}} + t_\parallel \sum_{\langle i\eta\rangle} c_\eta^\dagger c_i + \sum_{i,\mathbf{q}} M_{\mathbf{q}} c_i^\dagger c_i \mathrm{e}^{\mathrm{i}\mathbf{q}\cdot\mathbf{R}_i}(a_{\mathbf{q}} + a_{-\mathbf{q}}^\dagger),$$
$$\mathcal{H}_2 = \sum_j \epsilon^0 d_j^\dagger d_j + \sum_{\mathbf{p}} \hbar\omega_{\mathbf{p}} a_{\mathbf{p}}^\dagger a_{\mathbf{p}} + t_\parallel \sum_{\langle j\delta\rangle} d_\delta^\dagger d_j + \sum_{j,\mathbf{p}} M_{\mathbf{p}} d_j^\dagger d_j \mathrm{e}^{\mathrm{i}\mathbf{q}\cdot\mathbf{R}_j}(b_{\mathbf{p}} + b_{-\mathbf{p}}^\dagger),$$
$$\mathcal{H}_t = t_\perp \sum_i (c_i^\dagger d_i + \text{h.c.}).$$

Here, and below, $\mathbf{q}$, c, i, a, 1 refers to one layer and $\mathbf{p}$, d, j, b, 2 to the other one.

3. Small polarons

First we focus on the properties of the two layers separately, i.e., we ignore the term, $\mathcal{H}_t$, for the hopping between the layers. We perform a Lang–Firsov transformation [30] to diagonalize the Hamiltonian, excluding the hopping term, defined above, in each layer. Then $c_i \to \tilde{c}_i = c_i X_i$

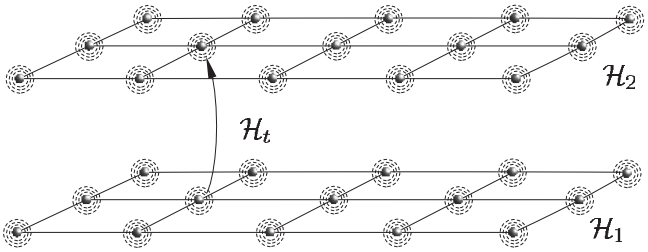

Figure 1. We model the two coupled layers as an anisotropic 3D system. Within each layer the electrons couple to bosons to potentially form small polarons. This is described by the Hamiltonians $\mathcal{H}_1$ and $\mathcal{H}_2$. The two layers are then coupled by a direct hopping term, $\mathcal{H}_t$.

and $d_j \to \tilde{d}_j = d_j Y_j$ where

$$\begin{aligned} X_i &= \exp\left[\sum_{\mathbf{q}} \mathrm{e}^{\mathrm{i}\mathbf{q}\cdot\mathbf{R}_i} \frac{M_{\mathbf{q}}}{\hbar\omega_{\mathbf{q}}}(a_{\mathbf{q}} - a^{\dagger}_{-\mathbf{q}})\right], \\ Y_j &= \exp\left[\sum_{\mathbf{p}} \mathrm{e}^{\mathrm{i}\mathbf{p}\cdot\mathbf{R}_j} \frac{M_{\mathbf{p}}}{\hbar\omega_{\mathbf{p}}}(b_{\mathbf{p}} - b^{\dagger}_{-\mathbf{p}})\right] \end{aligned} \tag{3}$$

are the polaron operators [20] for the first and second layer respectively. Further, $a_i \to a_i - \frac{M}{\omega_0} c_i^{\dagger} c_i$. The Hamiltonian is transformed to $\bar{\mathcal{H}} = \mathrm{e}^{S}\mathcal{H}\mathrm{e}^{-S}$ where $S = \frac{M}{\hbar\omega_0}\sum_i c_i^{\dagger}c_i(a_i^{\dagger} - a_i)$. The Hamiltonian becomes

$$\begin{aligned} \bar{\mathcal{H}} = &\sum_{\mathbf{q}} \hbar\omega_{\mathbf{q}} a^{\dagger}_{\mathbf{q}} a_{\mathbf{q}} + \sum_{\mathbf{p}} \hbar\omega_{\mathbf{p}} b^{\dagger}_{\mathbf{p}} b_{\mathbf{p}} - \sum_j \Delta d_j^{\dagger} d_j - \sum_i \Delta c_i^{\dagger} c_i \\ &+ t_{\parallel} \sum_{i,\eta} (c^{\dagger}_{i+\eta} c_i X^{\dagger}_{i+\eta} X_i + \text{h.c.}) + t_{\parallel} \sum_{j,\delta} (d^{\dagger}_{j+\delta} d_j Y^{\dagger}_{j+\delta} Y_j + \text{h.c.}) \\ &+ t_{\perp} \sum_{i,j} (c_i^{\dagger} d_j X_i^{\dagger} Y_j + \text{h.c.}), \end{aligned} \tag{4}$$

where

$$\Delta = \sum_{\mathbf{q}} \frac{M_{\mathbf{q}}^2}{\hbar\omega_{\mathbf{q}}} - \epsilon^0, \tag{5}$$

is the polaron binding energy. The intralayer hopping terms can be treated by adding to and subtracting from the Hamiltonian a term [31]

$$\mathcal{H}_{\mathrm{sp}} \equiv t_{\parallel} \sum_{\langle ij \rangle} \langle X_i X_j^{\dagger} \rangle c_i^{\dagger} c_j \equiv \sum_{\mathbf{k}} \epsilon_{\mathbf{k}} c^{\dagger}_{\mathbf{k}} c_{\mathbf{k}} \tag{6}$$

where $\langle \cdots \rangle$ denotes a thermal average over boson states and this term describes a tight binding band of small polarons for a square lattice within each layer [30, 31]:

$$\epsilon_{\mathbf{k}} = \epsilon^0 - \mathrm{e}^{-N^{-1}\sum_{\mathbf{q}} \left(\frac{M_{\mathbf{q}}}{\hbar\omega_{\mathbf{q}}}\right)^2 (1+2n_{\mathrm{B}})} t_{\parallel} [\cos(k_x a) + \cos(k_y a)], \tag{7}$$

where a is the lattice constant within the layers, N is the number of sites in one layer and $n_{\mathrm{B}}(T) = (\exp(\hbar\omega_{\mathbf{q}}/k_{\mathrm{B}}T) - 1)^{-1}$ is the Bose function. We see that the quasiparticles are described by a tight binding energy, where the bandwidth is reduced due to the polaron formation. Polaron transport narrowing has been seen experimentally in muon experiments [32].

There is then a residual interaction [31] between the polarons and the bosons which is described by

$$\bar{\mathcal{H}}_{p-b} = t_{\parallel} \sum_{\langle ij \rangle} [X_i X_j^{\dagger} - \langle X_i X_j^{\dagger} \rangle] c_i^{\dagger} c_j, \tag{8}$$

and leads to scattering of the small polarons.

3.1. Decay of the quasi-particles

Later we will need the decay, Γ, so we start by calculating it. We will calculate the first contribution to the self-energy in one layer by a method similar to the one used by Alexandrov and Mott [31]. The first non-zero contribution to the imaginary part of the self-energy, Σ, comes when the polaron emits one boson and absorbs one boson. This process is shown in figure 2, and is induced by the polaron–boson scattering from equation (8). By using Fermi's golden rule we get an expression for the decay:

$$\Gamma = 2\pi \sum_{\mathbf{q},\mathbf{q}'} |\langle n_{\mathbf{q}} - 1, n_{\mathbf{q}'+1}; \mathbf{k} + \mathbf{q} - \mathbf{q}' | \mathcal{H}_{p-b} | n_{\mathbf{q}}, n_{\mathbf{q}'}; \mathbf{k} \rangle|^2 \delta(\epsilon_{\mathbf{k}} - \epsilon_{\mathbf{k}+\mathbf{q}-\mathbf{q}'}). \tag{9}$$

Here, $\bar{\mathcal{H}}_{p-b}$ is the polaron–boson interaction in equation (8). Using this Hamiltonian we get that

$$\begin{aligned} &\langle n_{\mathbf{q}} - 1, n_{\mathbf{q}'+1}; \mathbf{k} + \mathbf{q} - \mathbf{q}' | \bar{\mathcal{H}}_{p-ph} | n_{\mathbf{q}}, n_{\mathbf{q}'}; \mathbf{k} \rangle \\ &\qquad = \frac{4t_{\parallel}}{N} \sqrt{n_{\mathbf{q}}} \sqrt{n_{\mathbf{q}'} + 1} \left(\frac{M_{\mathbf{q}}}{\hbar \omega_{\mathbf{q}}} \right) \left(\frac{M_{\mathbf{q}'}}{\hbar \omega_{\mathbf{q}'}} \right) \langle \mathbf{k} + \mathbf{q} - \mathbf{q}' | c_{\mathbf{k}+\mathbf{q}-\mathbf{q}'}^{\dagger} c_{\mathbf{k}} | \mathbf{k} \rangle \delta_{\mathbf{q}-\mathbf{q}'}. \end{aligned} \tag{10}$$

To simplify this to get an energy independent expression we use an energy independent density of states and assume a $\mathbf{k}$ independent coupling between the electrons and the bosons. We only consider a single frequency ω_0 for reasons of simplicity; this allows us to express some of our results in an analytical form. Then we can define the dimensionless coupling

$$g \equiv \left(\frac{M}{\hbar \omega_0} \right)^2 \tag{11}$$

that will enter our equations later. We require that g is greater than or equal to 1 in order for small polaronic effects to be important[2]. Using this, we get that

$$\tau^{-1} = W g^2 n_{\mathrm{B}} (1 + n_{\mathrm{B}}), \tag{12}$$

where $W = 4\tilde{t}_{\parallel}$ is the polaron bandwidth, which is subject to narrowing due to the renormalization of the hopping $t \to \tilde{t}_{\parallel} \equiv t_{\parallel} \mathrm{e}^{-g(1+2n_{\mathrm{B}})}$.

3.2. The Green function in the layer

Let us start by calculating the retarded *electron* Green function (GF) within one layer, ignoring the coupling between the layers ($t_{\perp} = 0$). This gives us valuable information on the coherence of the quasi-particles, and can be compared to angle resolved photoemission spectra (ARPES). After performing the Lang–Firsov transformation the small polaron GF is

$$G^0(\mathbf{k}, \tau) = -\mathrm{i}\Theta(\tau) \frac{1}{N} \sum_{i,i'} \mathrm{e}^{\mathrm{i}\mathbf{k}\cdot(\mathbf{R}_i - \mathbf{R}_{i'})} \langle T_{\tau} c_i(\tau) c_{i'}^{\dagger}(0) \rangle = -\mathrm{i}\Theta(\tau) \mathrm{e}^{(\epsilon_{\mathbf{k}} - \mathrm{i}\Gamma)\mathrm{i}\tau/h}. \tag{13}$$

[2] Strictly speaking there are three conditions for small polaron transport [29], $t < g\hbar\omega_0$, $\sqrt{2}t < M$ and $t < \sqrt{M}(\frac{2k_{\mathrm{B}}T\hbar\omega_0}{\pi^3})^{1/4}$.

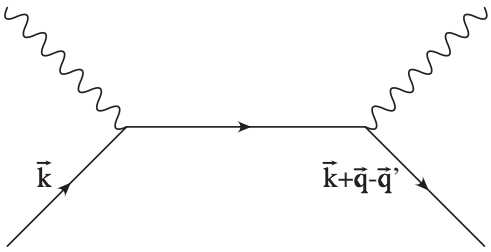

Figure 2. The diagram describing the first contribution to the polaron decay, Γ. The polaron emits and absorbs one boson, changing its momenta.

Γ is the imaginary part of the polaron self-energy. In this equation we have ignored the real part of the self-energy since we will use a model dispersion anyway. To get the electron GF we have to convolute this GF with the average over two polaron operators $\langle T X_i^\dagger(t) X_{i'}(0)\rangle \equiv \Phi_{ii'}(t)$. This average can be decoupled and written as an exponential [30, 20]:

$$\Phi_{ii'}(t) = \mathrm{e}^{-g(1/2+n_\mathrm{B})} \exp\left\{ g \sum_{\mathbf{q}} \cos[\mathbf{q}\cdot(\mathbf{R}_i - \mathbf{R}_{i'})][(1+n_\mathrm{B})\mathrm{e}^{-\mathrm{i}\omega t} + n_\mathrm{B}\mathrm{e}^{\mathrm{i}\omega t}] \right\}. \tag{14}$$

After Fourier transforming the average of the polaron operators, giving a sum of delta functions, we will have a convolution

$$G(\mathbf{k}, \mathrm{i}\omega_n) = \frac{1}{N} \sum_{\omega_{n'}, \mathbf{R}_m, \mathbf{k}'} \Phi(\mathbf{R}_m, \omega_{n'} - \omega_n) G^0(\mathbf{k}', \omega_{n'}) \mathrm{e}^{\mathrm{i}(\mathbf{k}-\mathbf{k}')\cdot\mathbf{R}_m}. \tag{15}$$

After some algebra we come to the following expression:

$$G(\mathbf{k}, \mathrm{i}\omega_n) = \mathrm{e}^{-g(1+2n_\mathrm{B})} \frac{1}{N} \sum_{\mathbf{R}_m, \mathbf{k}'} \mathrm{e}^{\mathrm{i}(\mathbf{k}-\mathbf{k}')\cdot\mathbf{R}_m} \sum_{l=-\infty}^{\infty} \frac{I_l[2g\sum_{\mathbf{q}} \cos(\mathbf{q}\cdot\mathbf{R}_m)\sqrt{n_\mathrm{B}(1+n_\mathrm{B})}]\mathrm{e}^{-l\hbar\omega_0\beta/2}}{\mathrm{i}\omega_n - \epsilon_{\mathbf{k}'} + l\hbar\omega_0 + \mathrm{i}\Gamma}. \tag{16}$$

Here I_l indicates a modified Bessel function of order l. Performing the summation over $\mathbf{R}_m$, care has to be taken when considering the $l = 0$ term; we get the final result for the GF:

$$G(\mathbf{k}, \omega) = \mathrm{e}^{-g(1+2n_\mathrm{B})} \left\{ \frac{1}{\omega - \epsilon_{\mathbf{k}} + \mathrm{i}\Gamma} + \sum_{\mathbf{k}'} \frac{I_0[2g\sqrt{n_\mathrm{B}(1+n_\mathrm{B})}] - 1}{\omega - \epsilon_{\mathbf{k}'} + \mathrm{i}\Gamma} \right.$$
$$\left. + \sum_{\mathbf{k}', l\neq 0} \frac{I_l[2g\sqrt{n_\mathrm{B}(1+n_\mathrm{B})}]\mathrm{e}^{-l\hbar\omega_0\beta/2}}{\omega - \epsilon_{\mathbf{k}'} + l\hbar\omega_0 + \mathrm{i}\Gamma} \right\}. \tag{17}$$

Note that we have written the GF as a sum of a coherent and an incoherent part. This can be compared to the zero-temperature result given by Alexandrov and Mott [31]. At $T = 0$ there are no bosons to absorb and only $l \geqslant 0$ contributes to the GF. Also, we can compare this to the non-zero temperature GF given by Ciuchi *et al* [33]. The first line is dependent on $\mathbf{k}$, thereby describing a coherent part. There will be a well-defined quasiparticle peak at $\omega = \epsilon_{\mathbf{k}}$, with a spectral weight of $\mathrm{e}^{-g(1+2n_\mathrm{B})}$. The second and third lines contain a sum over the intralayer momentum and are therefore independent of $\mathbf{k}$; they are incoherent. The two contributions have different temperature dependences: the coherent one dominates at low temperature and the incoherent one at high temperature. This means that there is a crossover from coherent intralayer motion at low temperature to incoherent intralayer motion at high temperatures. In figure 3 we show the spectral function resulting from this GF at the Fermi wavevector as a function of the energy. The summation over $\mathbf{k}$ is done by integrating over

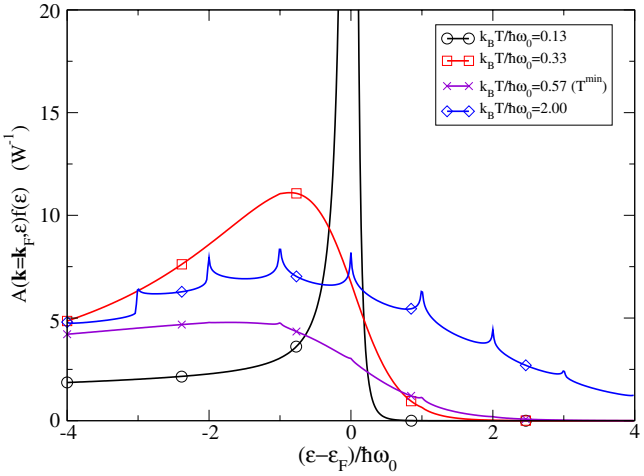

Figure 3. The quasi-particle spectral function, $n_f(\epsilon)\,\mathrm{Im}[G(\mathbf{k}_\mathrm{F},\epsilon)]$, for an electron–phonon coupling, $g = 1$, for different temperatures. The sum over $\mathbf{k}$ is done by integrating over the density of states, which we assume is flat with a bandwidth $W = 77\hbar\omega_0$. There are two contributions to the spectral function, one coherent, dominating at low temperatures, and one incoherent, dominating at high temperatures. Similar behaviour has been seen experimentally [4].

a flat density of states. This is what is measured in ARPES experiments such as the one in [4] for $(Bi_{0.5}Pb_{0.5})_2Ba_3Co_2O_y$ and $NaCo_2O_4$. Recently, similar features were seen for Sr_2RuO_4 [34]. The coherent contribution displays a peak at the Fermi energy and the $\mathbf{k}$ vector at low temperature, indicating a coherent quasi-particle. The peak disappears as the temperature is increased. From plots of the spectral function one can estimate a crossover temperature when the contribution from the incoherent part starts to dominate over the incoherent one. This will take place when

$$k_\mathrm{B}T^\mathrm{coh} \sim \frac{\hbar\omega_0}{2g}. \tag{18}$$

Note that coherent quasiparticles are still present in the spectral function; it is just that at the Fermi level there are more incoherent ones. It is hard to find a precise measure of the crossover, since it depends on what measurements are made and how they relate to the spectral function; e.g., for the conductivity it is an integrated quantity with a spread around the Fermi level depending on the temperature. Later we will see that the drop in coherent quasiparticles is related to the interlayer conductivity.

4. Transport properties

Let us now turn to the transport properties of the layered material which is described by the layered Hamiltonian defined above. At an applied voltage V, the current is given by the current–current correlation function derived from the Kubo formula [20]

$$I_{\mu\nu}(eV) = \frac{2e}{h}\,\mathrm{Im}\left\{\int_0^\beta \mathrm{d}t\,\mathrm{e}^{\mathrm{i}eVt}\langle T\,\hat{j}_\mu(t)\hat{j}_\nu^\dagger(0)\rangle\right\}, \tag{19}$$

where $\hat{j}$ is the current operator. μ and ν are directions in the crystal. For our system, including polarons, the current operator for nearest neighbour hopping is

$$(j_a, j_b, j_c) = -\frac{\mathrm{i}e}{\hbar}\Bigg[t_\parallel \sum_{i,\eta}(\vec{R}^\parallel_{i+\eta} - \vec{R}^\parallel_i)c^\dagger_{i+\eta}c_i X^\dagger_{i+\eta}X_i + t_\parallel \sum_{j,\eta}(\vec{R}^\parallel_{j+\eta} - \vec{R}^\parallel_j)d^\dagger_{j+\eta}d_j Y^\dagger_{j+\eta}Y_j + t_\perp \sum_{j,\delta}(\vec{R}^\perp_{j+\delta} - \vec{R}^\perp_j)d^\dagger_{j+\delta}c_j Y^\dagger_{j+\delta}X_j\Bigg]. \tag{20}$$

The first term corresponds to hopping in layer 1, the second term to hopping in layer 2 and the third to hopping between adjacent positions in the two layers. Since we also are going to study thermopower, we give the expression for the energy current in the same model:

$$(j^e_a, j^e_b, j^e_c) = -\frac{\mathrm{i}e}{\hbar}\Bigg[\frac{t_\parallel\epsilon}{2} \sum_{i,\eta}(\vec{R}^\parallel_{i+\eta} - \vec{R}^\parallel_i)c^\dagger_{i+\eta}c_i X^\dagger_{i+\eta}X_i + \frac{t_\parallel\epsilon}{2} \sum_{j,\eta}(\vec{R}^\parallel_{j+\eta} - \vec{R}^\parallel_j)d^\dagger_{j+\eta}d_j Y^\dagger_{j+\eta}Y_j + \frac{t_\perp\epsilon}{2} \sum_{j,\delta}(\vec{R}^\perp_{j+\delta} - \vec{R}^\perp_j)d^\dagger_{j+\delta}c_j Y^\dagger_{j+\delta}X_j\Bigg], \tag{21}$$

and ϵ is the energy of the quasi-particle. Let us separate the current within the layers and perpendicular to the layers, since they usually show different behaviours in experiment.

4.1. Current within the layers

In this section we will calculate the current within the layers. We split the calculation into two regimes because if we use equation (20) directly in equation (19), the result is too complicated to decouple, so we split the calculation into low and high temperature parts, where different parts of the Hamiltonian dominate, and we can use perturbation theory.

4.1.1. Low temperatures. At low temperatures the transport within the layers is coherent. If the layers are metallic we can treat them in a Fermi liquid manner and use that the conductivity depends on the scattering rate via the scattering time, $\tau = h/\Gamma$:

$$\sigma_\parallel = \frac{e^2}{2\pi^2}\int v(\mathbf{k})\bar{v}(\mathbf{k})\left(-\frac{\partial f}{\partial\epsilon}\right)\tau(\mathbf{k})\,\mathrm{d}^2k. \tag{22}$$

The decay is calculated as usual from the imaginary part of the self-energy, and is given in equation (12). We use the tight binding approximation, equation (7), to get the quasiparticle velocity, $\mathbf{v}(\mathbf{k}) = \frac{\nabla_\mathbf{k}\epsilon_\mathbf{k}}{\hbar}$, in one direction and get the conductivity,

$$\sigma^{xx}_\parallel = \frac{e^2}{\pi h}\frac{\beta\tilde{t}_\parallel a^2}{g^2 n_\mathrm{B}(1+n_\mathrm{B})}\int_{-2\pi}^{2\pi}\mathrm{d}x\,\mathrm{d}y\,\frac{\sin^2(x)}{1+\cosh[\beta(\epsilon_0+\tilde{t}_\parallel\cos(x)+\tilde{t}_\parallel\cos(y)-\mu)]}. \tag{23}$$

4.1.2. High temperatures. At high temperatures the polarons are localized, the bandwidth disappears and the hopping, $t_\parallel$, is the perturbation. Utilizing equation (19) for the current, we decouple the electron operators to polaron GFs in each layer, $G = (\omega - \Delta + \Sigma + \mathrm{i}\Gamma)^{-1}$. Note that there is no $\mathbf{k}$ dependence for the polaron GFs since they are localized at an energy $\Delta = \epsilon_0 - g\hbar\omega_0 < 0$. The calculation of the GF in perturbation theory is described in the appendix. The four X operators are decoupled as in [20] into diagonal (no change of boson state) and non-diagonal transitions (when the boson state changes in the hop). The result for the non-diagonal transitions is

$$\langle T_\tau X^\dagger(\tau)X(\tau)X^\dagger(0)X(0)\rangle_\omega = \mathrm{e}^{-2g(1+2n_\mathrm{B})}\sum_{l=-\infty}^{\infty}\left\{\int_{-\infty}^{\infty} I_l\big[4g\sqrt{n_\mathrm{B}(1+n_\mathrm{B})}\big]\mathrm{e}^{-l\hbar\omega_0\beta/2}\mathrm{e}^{\mathrm{i}l\omega_0 t} - 1\right\}. \tag{24}$$

For the diagonal part, the four X operators decouple and cancel the -1 term above when added together. Combining the two correlators and taking the imaginary part we convolute the two Fourier transforms similarly to what was done for the GF above, so we get for the current

$$I_{\parallel}(\omega) = \frac{2e}{h} t_{\parallel}^2 d^2 \mathrm{e}^{-2g(1+2n_{\mathrm{B}})} \int_{-\infty}^{\infty} \frac{\mathrm{d}\epsilon}{2\pi} A(\epsilon) \times \sum_{l=-\infty}^{\infty} I_l\left[4g\sqrt{n_{\mathrm{B}}(1+n_{\mathrm{B}})}\right] \mathrm{e}^{-l\hbar\omega_0\beta/2} A(\epsilon+\omega+l\hbar\omega_0) \times [n_{\mathrm{F}}(\epsilon) - n_{\mathrm{F}}(\epsilon+\omega+l\hbar\omega_0)]. \tag{25}$$

The conductance is obtained as usual as $\sigma_{\parallel} = e\frac{\mathrm{d}I_{\parallel}}{\mathrm{d}(\omega)}|_{\omega=0}$.

The conductivity can now be plotted. The metallic, low temperature, part decreases with increasing temperature and the insulating, high temperature, phase takes over as temperature is increased. There is a peak in the resistivity and a crossover from coherent to incoherent transport, described by equations (23) and (25) respectively. We constructed similar plots for a range of coupling constants, g, and saw that the intralayer crossover occurs at a temperature given by

$$k_{\mathrm{B}} T_{\parallel}^{\max} \sim 2\frac{\hbar\omega_0}{g}. \tag{26}$$

We have used the same decay, Γ, for both the low and high temperature limits. This approximation assumes that the dominant part of the scattering of the carriers in both limits is the electron–boson coupling. The results are shown in the figures below.

4.2. Current perpendicular to the layers

Let us now turn to the current perpendicular to the layers. The current operator for an applied field in the perpendicular direction in a nearest neighbour hopping model (from layer 1 to 2) is given in equation (20). We assume that the hopping between the layers only take place between nearest neighbours; see figure 1. Then, $(\mathbf{R}_{j+\delta} - \mathbf{R}_j)$ is the distance between the two layers, d, since $\delta = 1$ for nearest neighbour hopping. The Kubo formula, equation (19), gives, to second order in $t_{\perp}$,

$$I_{\perp}(eV) = \frac{2e}{h} t_{\perp}^2 d^2 \sum_{j,j_1} \int_0^{\beta} \mathrm{d}\tau\, \mathrm{e}^{\mathrm{i}eV\tau} \langle T_\tau c_j^{\dagger}(\tau) d_{j_1}(\tau) d_j^{\dagger}(0) c_{j_1}(0)\rangle \langle T_\tau Y_{j_1}^{\dagger}(\tau) Y_j(\tau) X_j^{\dagger}(0) X_{j_1}(0)\rangle. \tag{27}$$

We decouple the operators in the first and second layer. This means that the Fourier transformed averages of the electron operators give rise to polaron Green functions:

$$\langle T c_j^{\dagger}(t) c_{j_1}(0)\rangle \to G_1^0(\mathbf{k}, \mathrm{i}p_n),$$
$$\langle T d_{j_1}(t) d_j^{\dagger}(0)\rangle \to G_2^0(\mathbf{p}, \mathrm{i}p_n - \mathrm{i}\omega).$$

The average of the polaron operators (X, Y) can be decoupled for the two layers separately, and written as an exponential $\Phi(t)$ [30, 20], as was done for the GF above. Since the couplings in all layers are the same, $M_1 = M_2$, we can either combine the two averages of the polaron operators into one exponential $(\Phi(t) * \Phi(t) = (\Phi(t))^2)$ or keep them as two separate ones. Then we can perform the Fourier transform $\tau \to \omega$, and if we assume that the GF has an imaginary part, as above, we get the following for the interlayer tunnelling current:

$$I_{\perp}(eV) = \frac{2e}{h} t_{\perp}^2 d^2 \mathrm{e}^{-2g(1+2n_{\mathrm{B}})} \left\{ \int_{-\infty}^{\infty} \frac{\mathrm{d}\epsilon}{2\pi} \sum_{\mathbf{k}} A_1^0(\mathbf{k}, \epsilon) A_2^0(\mathbf{k}, \epsilon + eV)[f(\epsilon) - f(\epsilon + eV)] \right.$$

$$+\left(I_0\left[4g\sqrt{n_{\mathrm{B}}(1+n_{\mathrm{B}})}\right]-1\right)\int_{-\infty}^{\infty}\frac{\mathrm{d}\epsilon}{2\pi}\sum_{\mathbf{k}}A_1^0(\mathbf{k},\epsilon)\sum_{\mathbf{p}}A_2^0(\mathbf{p},\epsilon+eV)$$
$$\times\left[f(\epsilon)-f(\epsilon+eV)\right]+\sum_{\substack{l\neq 0\\ l=-\infty}}^{\infty}I_l\left[4g\sqrt{n_{\mathrm{B}}(1+n_{\mathrm{B}})}\right]\mathrm{e}^{-l\hbar\omega_0\beta/2}$$
$$\times\int_{-\infty}^{\infty}\frac{\mathrm{d}\epsilon}{2\pi}\sum_{\mathbf{k}}A_1^0(\mathbf{k},\epsilon)\sum_{\mathbf{p}}A_2^0(\mathbf{p},\epsilon+eV+l\hbar\omega_0)$$
$$\times\left[f(\epsilon)-f(\epsilon+eV+l\hbar\omega_0)\right]\Bigg\} \tag{28}$$

$\mathbf{k}$ belongs to the first layer and $\mathbf{p}$ to the second. A_1^0 and A_2^0 are the spectral functions for the electron GFs in each layer:

$$A_1^0(\mathbf{k},\epsilon)=\frac{\Gamma}{(\epsilon-\epsilon_{\mathbf{k}})^2+\Gamma^2}, \tag{29}$$

$$A_2^0(\mathbf{p},\epsilon)=\frac{\Gamma}{(\epsilon-\epsilon_{\mathbf{p}})^2+\Gamma^2}. \tag{30}$$

The index l is a combined index—for the number of bosons emitted or absorbed in layers 1 and 2 combined.

To illustrate this, consider what would be obtained if we had not combined the two exponentials; the result would be

$$I_\perp(eV)\propto 2t_\perp^2\mathrm{e}^{-\sum_{\mathbf{q}}(\frac{M_{\mathbf{q}}}{\hbar\omega_{\mathbf{q}}})^2(1+2n_{\mathrm{B}})-\sum_{\mathbf{p}}(\frac{M_{\mathbf{p}}}{\hbar\omega_{\mathbf{p}}})^2(1+2n_{\mathrm{B}})}$$
$$\times\prod_{\mathbf{q},\mathbf{p}}\sum_{l,l'=-\infty}^{\infty}\int_{-\infty}^{\infty}\frac{\mathrm{d}\epsilon}{2\pi}A_2(\epsilon-l'\hbar\omega_{\mathbf{q}})A_1(\epsilon+eV+l\hbar\omega_{\mathbf{p}})$$
$$\times\left[n_{\mathrm{F}}(\epsilon-l'\hbar\omega_{\mathbf{q}})-n_{\mathrm{F}}(\epsilon+eV+l\hbar\omega_{\mathbf{p}})\right]$$
$$\times I_l\left(2\left(\frac{M_{\mathbf{p}}}{\hbar\omega_{\mathbf{p}}}\right)^2\sqrt{n_{\mathrm{B}}(1+n_{\mathrm{B}})}\right)I_{l'}\left(2\left(\frac{M_{\mathbf{q}}}{\hbar\omega_{\mathbf{q}}}\right)^2\sqrt{n_{\mathrm{B}}(1+n_{\mathrm{B}})}\right)\mathrm{e}^{-\beta/2(l\hbar\omega_{\mathbf{p}}+l'\hbar\omega_{\mathbf{q}})}. \tag{31}$$

l belongs to the first layer and counts the number of bosons attached to the electron; l' refers in a similar fashion to the second layer. The connection between equations (28) and (31) can be found from the identity for the Bessel functions

$$\sum_{l,l'=-\infty}^{\infty}I_{l-l'}(x_1)I_{l'}(x_2)=\sum_{l=-\infty}^{\infty}I_l(x_1+x_2). \tag{32}$$

Equation (28) describes the polaron jumping and the shift in phonons attached to the polaron in the jump, whereas equation (31) describes the electron and its attached phonon cloud in each layer, l and l' respectively.

The expression for the current, equation (28), has one contribution from coherent and two from incoherent transport. Note the similarity of the structure of equation (28) to that of the expression for the GF, equation (17). The first term corresponds to transport which conserves the intralayer momentum in the tunnelling process. This is seen since the crystal momentum $\mathbf{k}$ is the same for the spectral function for the two different layers. For the other terms, the intralayer momentum is not conserved (in each layer the sums over the momentum are separate). The second row corresponds to transport when the net number of bosons in the system is unchanged. When the quasi-particle tunnels it leaves behind the cloud of bosons

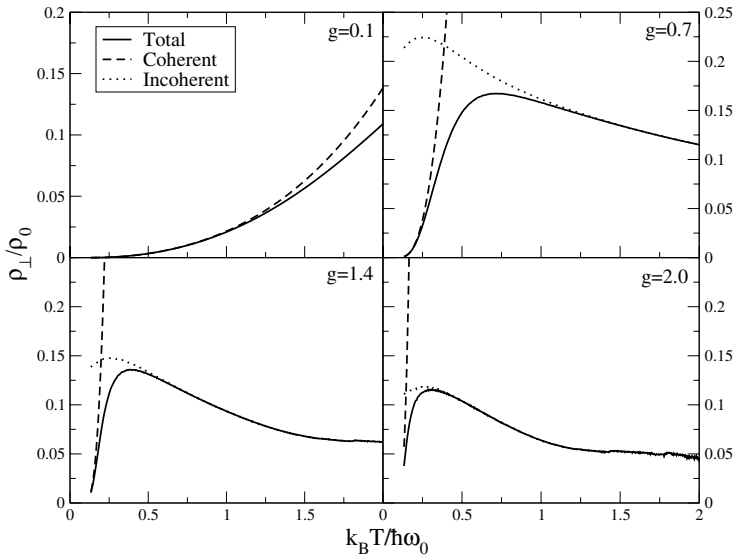

Figure 4. Interlayer resistivity as a function of temperature for different values of the coupling g. At low temperatures, the transport is predominantly coherent, as seen from equation (28). Then, as the temperature is increased, the incoherent mechanism of transport takes over. We have $\sigma_\perp = \sigma_\perp^{\text{coh.}} + \sigma_\perp^{\text{inc.}}$; the two contributions are shown separately and together in the plot. The crossover from coherent to incoherent transport is clearly seen. $\rho_0^{-1} = \frac{2e^2}{\hbar} t_\perp^2 d^2$, $W = 77\hbar\omega_0$.

in one layer and attaches to a replica of bosons in the second layer. The third row describes transport when a net number of bosons is absorbed ($l > 0$) or emitted ($l < 0$), thus changing the energy of the polaron in the hop between the two layers. In a recent paper [28] we established a connection between the intralayer coherence and the appearance of dips in the angular magnetoresistance, the so-called 'magic angles'. We showed that a contribution from incoherent jumps between highly conducting one-dimensional strands of molecules gives a natural explanation of the phenomena observed in the magnetoresistance. At low temperature the coherent part dominates but at high temperature (high compared to the boson energy, $\hbar\omega_0$, $k_B T > \hbar\omega_0$) the incoherent mechanism of transport will dominate. Thus, there is a *crossover* from coherent to incoherent transport. The crossover temperature is fixed by having equal contributions from the coherent and the incoherent parts. Ignoring the contribution from the $l \neq 0$ terms in equation (28) we can get an approximate expression for the crossover temperature:

$$k_B T_\perp^{\max} \sim \frac{\hbar\omega_0}{\sqrt[4]{2^3}\, g} \sim 1.68 \frac{\hbar\omega_0}{g}. \tag{33}$$

From equation (28) we can extract the conductivity via a simple derivative: $\sigma_\parallel = e \frac{\mathrm{d}I_\parallel}{\mathrm{d}(eV)}|_{eV=0}$. In figure 4 we plot the conductivity as a function of temperature for one value of g. The crossover is clearly seen.

In general, the interlayer conductivity for identical decoupled layers is [35]

$$\sigma_\perp = \frac{2e^2}{h} t_\perp^2 \int \mathrm{d}\epsilon \sum_{\mathbf{k}} |A(\mathbf{k}, \epsilon)|^2 \left[-\frac{\mathrm{d}f}{\mathrm{d}\epsilon} \right], \tag{34}$$

where $A(\mathbf{k}, \epsilon)$ is the *electron* spectral function for a single layer. Directly substituting equation (17) in (34) we obtain the same result as was found from equation (28).

We can check the result by taking some limits in equation (28). When the temperature is zero, we get

$$\sigma_\perp(T=0) = \frac{2e^2}{h} t_\perp^2 d^2 \mathrm{e}^{-2g} \sum_{\mathbf{k}} \frac{A_1(\mathbf{k},0)A_2(\mathbf{k},0)}{2\pi} = \frac{2e^2}{2\pi h} t_\perp^2 \mathrm{e}^{-2g} \frac{D(\epsilon=0)}{2\Gamma}. \tag{35}$$

Here, $D(\epsilon = 0)$ is the density of states at the Fermi level. Thus, at low temperature when only the first (coherent) term contributes to the conductivity, the temperature dependence of $\sigma_\perp$ is governed by the temperature dependence of the decay, Γ, given by equation (12), for the polaron case. If we expand equation (28) for high temperatures the conductivity behaves approximately as

$$\sigma_\perp \propto T^{-3/2}, \tag{36}$$

which is consistent with the equipartition theorem [36]. In figure (4) this should be an upturn in the resistivity; it is not seen for $g > 0.1$, since it happens first when $k_\mathrm{B}T/\hbar\omega_0 \gg 2$, i.e., after we cut the plot.

If we take the limit $g = 0$ we get

$$\sigma_\perp(g=0) = \frac{2e^2}{h} t_\perp^2 d^2 \sum_{\mathbf{k}} \int_{-\infty}^{\infty} \frac{\mathrm{d}\epsilon}{2\pi} A_1(\mathbf{k},\epsilon)A_2(\mathbf{k},\epsilon)\beta n_\mathrm{F}(\epsilon)[1-n_\mathrm{F}(\epsilon)], \tag{37}$$

as expected from transport theory [20].

4.3. Thermopower

Let us now turn to calculating the thermopower for intralayer and interlayer transport. The thermopower is defined as a correlator, using the heat current instead of the electrical current in equation (19) (see [20]):

$$L^{12} = \frac{2e}{h} \mathrm{Im}\left\{ \int_0^\beta \mathrm{d}t\, \mathrm{e}^{\mathrm{i}\omega t} \langle T\, \hat{j}_\mu^e(t)\, \hat{j}_\nu^\dagger(0)\rangle \right\}, \tag{38}$$

and, using that the current–current correlator gives us L^{11}, and $\sigma = L^{11}/T$, we get

$$S = \frac{1}{T}\frac{L^{12}}{L^{11}} = \frac{1}{T^2}\frac{L^{12}}{\sigma}. \tag{39}$$

For the intralayer thermopower we consider the low and high temperature limits separately.

4.3.1. Low temperature intralayer thermopower. At low temperatures the correlator is similar to the one calculated for the intralayer low temperature conductivity, except for an additional $\epsilon_k/2$ in the (energy) current operator. This factor only contributes an additional $\tilde{t_\parallel}\cos(k_x a)/2$ if we assume that we do the measurement along x. The result is that, for low temperatures, the thermopower is

$$S_\parallel^{\mathrm{low}} = \frac{1}{T}\frac{\tilde{t_\parallel}}{2e} \frac{\int \mathrm{d}^2k\, f(\epsilon_\mathbf{k})[1-f(\epsilon_\mathbf{k})]\sin^2(k_x a)\cos(k_x a)}{\int \mathrm{d}^2k\, f(\epsilon_\mathbf{k})[1-f(\epsilon_\mathbf{k})]\sin^2(k_x a)}. \tag{40}$$

4.3.2. High temperature intralayer thermopower. At high temperatures, we can follow the same steps as for the intralayer current, with the only difference that the energy operator is the current operator multiplied by $\frac{t_\parallel}{2}$. Then, in equation (39) the correlators cancel, and we simply end up with [37]

$$S_\parallel^{\mathrm{high}} = \frac{t_\parallel}{2eT}. \tag{41}$$

The thermopower in the high temperature limit falls off as $\frac{1}{T}$. In the low temperature limit, there is a prefactor of $\frac{1}{T}$ in equation (40), but the magnitude depends heavily on the filling of the polaron band. The two results in the low and high temperature regions, equations (40) and (41) respectively, have a strong $\frac{1}{T}$ dependence. This means that there does not necessarily have to be a peak in the intralayer thermopower corresponding to any transition between coherent and incoherent transport. Therefore, the transition in the intralayer transport is more clearly seen in the electrical transport, not the thermopower. The $1/T$ dependence is typical for polarons at high temperatures as seen, e.g., in $La_{2/3}Ca_{1/3}MnO_3$ films [38] and (La, Ca)MnO_3 [12].

4.3.3. Interlayer thermopower. We follow the same steps as for the interlayer conductivity with the replacement of one current operator by one energy–current operator as in equation (38). The result for L^{12} is

$$\begin{aligned} L_\perp^{12} = \frac{2e}{h} t_\perp^2 \mathrm{e}^{-2g(1+2n_\mathrm{B})} d^2 \Bigg\{ & \int_{-\infty}^{\infty} \frac{\mathrm{d}\epsilon}{2\pi} \sum_{\mathbf{k}} \xi_{\mathbf{k}} A_1^0(\mathbf{k},\epsilon) A_2^0(\mathbf{k},\epsilon+eV)[f(\epsilon)-f(\epsilon+eV)] \\ & + \left(I_0\left[4g\sqrt{n_\mathrm{B}(1+n_\mathrm{B})}\right]-1\right) \\ & \times \int_{-\infty}^{\infty} \frac{\mathrm{d}\epsilon}{2\pi} \sum_{\mathbf{k}} \xi_{\mathbf{k}} A_1^0(\mathbf{k},\epsilon) \sum_{\mathbf{p}} A_2^0(\mathbf{p},\epsilon+eV)[f(\epsilon)-f(\epsilon+eV)] \\ & + \sum_{\substack{l\neq 0 \\ l=-\infty}}^{\infty} I_l\left[4g\sqrt{n_\mathrm{B}(1+n_\mathrm{B})}\right] \mathrm{e}^{-l\hbar\omega_0\beta/2} \int_{-\infty}^{\infty} \frac{\mathrm{d}\epsilon}{2\pi} \sum_{\mathbf{k}} \xi_{\mathbf{k}} A_1^0(\mathbf{k},\epsilon) \\ & \times \sum_{\mathbf{p}} A_2^0(\mathbf{p},\epsilon+eV+l\hbar\omega_0)[f(\epsilon)-f(\epsilon+eV+l\hbar\omega_0)] \Bigg\}. \end{aligned} \tag{42}$$

Here $\xi_{\mathbf{k}} = \epsilon_{\mathbf{k}} - \mu$. The thermopower is then given by equation (39). In figure 5 we make a comparative plot of the resistivity and the thermopower between the layers. For a Fermi liquid the thermopower would fall off as $\frac{1}{T}$ at high temperatures (see, e.g., Salamon *et al* [11]); fitting a curve to our numerical results shows that our expression for the interlayer thermopower falls off *exponentially* instead.

4.4. Optical conductivity

The optical conductivity is given by calculating the derivative of the frequency dependent current $I_\perp(\omega)$ in equation (28) with respect to $\omega = eV$. We assume that the following relations hold (when $\Gamma \ll W$):

$$\int \mathrm{d}x\, D(x) A(x,\epsilon) = \int \mathrm{d}x\, D(x) \frac{\Gamma}{(\epsilon-x)^2+\Gamma^2} = D(\epsilon),$$

$$\begin{aligned} & \int \mathrm{d}x\, D(x) A(x,\epsilon) A(x,\epsilon+\omega) \\ & \qquad = \int \mathrm{d}x\, D(x) \frac{\Gamma}{(\epsilon-x)^2+\Gamma^2} \frac{\Gamma}{(\epsilon+\omega-x)^2+\Gamma^2} = D(\epsilon) \frac{\Gamma}{\omega^2+\Gamma^2}. \end{aligned}$$

We get that the full expression for the optical conductivity is

$$\begin{aligned} \sigma(\omega) = \frac{2e^2}{h} t_\perp^2 d^2 \mathrm{e}^{-2g(1+2n_\mathrm{B})} \Bigg\{ & \int_{-\infty}^{\infty} \frac{\mathrm{d}\epsilon}{2\pi} D(\epsilon) \frac{\Gamma}{\omega^2+\Gamma^2} \beta n_\mathrm{F}(\epsilon+\omega)[1-n_\mathrm{F}(\epsilon+\omega)] \\ & + \left(I_0\left[4g\sqrt{n_\mathrm{B}(1+n_\mathrm{B})}\right]-1\right) \int_{-\infty}^{\infty} \frac{\mathrm{d}\epsilon}{2\pi} D(\epsilon) D(\epsilon+\omega) \beta n_\mathrm{F}(\epsilon+\omega) \end{aligned}$$

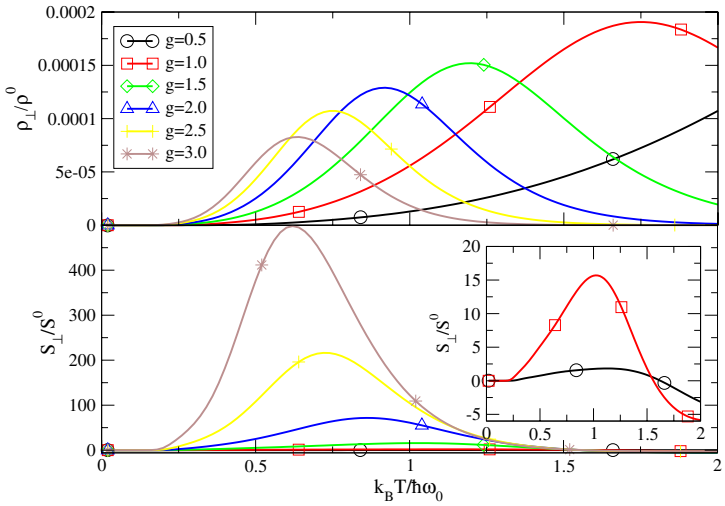

Figure 5. The top panel shows the interlayer resistivity as a function of temperature for different electron–phonon coupling strengths, $\rho_0^{-1} = \frac{2e^2}{\hbar} t_\perp^2 d^2$, $W = 160\hbar\omega_0$. The peak corresponds to the transition between coherent and incoherent transport. The lower panel shows the interlayer thermopower, $S^0 = \frac{t_\perp}{2e}$. The peak in the thermopower occurs at a lower temperature than for the resistivity. The inset shows the thermopower for small electron–phonon coupling; note that it can change sign although we do not consider carriers of hole type here. At high temperatures, and strong electron–phonon coupling, the thermopower decays exponentially.

$$
\begin{aligned}
&\times [1 - n_{\mathrm{F}}(\epsilon + \omega)] + \sum_{l=-\infty}^{\infty} I_l\big[4g\sqrt{n_{\mathrm{B}}(1+n_{\mathrm{B}})}\big] \mathrm{e}^{-l\hbar\omega_0\beta/2} \\
&\times \int_{-\infty}^{\infty} \frac{\mathrm{d}\epsilon}{2\pi} D(\epsilon) D(\epsilon + \omega + l\hbar\omega_0) \\
&\times \beta n_{\mathrm{F}}(\epsilon + \omega + l\hbar\omega_0)[1 - n_{\mathrm{F}}(\epsilon + \omega + l\hbar\omega_0)] \\
&+ \int_{-\infty}^{\infty} \frac{\mathrm{d}\epsilon}{2\pi} D(\epsilon) \frac{2\Gamma\omega}{(\omega^2 + \Gamma^2)^2} [n_{\mathrm{F}}(\epsilon) - n_{\mathrm{F}}(\epsilon + \omega)] \\
&+ \Big(I_0\big[4g\sqrt{n_{\mathrm{B}}(1+n_{\mathrm{B}})}\big] - 1\Big) \int_{-\infty}^{\infty} \frac{\mathrm{d}\epsilon}{2\pi} D(\epsilon) D'(\epsilon + \omega)[n_{\mathrm{F}}(\epsilon) - n_{\mathrm{F}}(\epsilon + \omega)] \\
&+ \sum_{l=-\infty}^{\infty} I_l\big[4g\sqrt{n_{\mathrm{B}}(1+n_{\mathrm{B}})}\big] \mathrm{e}^{-l\hbar\omega_0\beta/2} \int_{-\infty}^{\infty} \frac{\mathrm{d}\epsilon}{2\pi} D(\epsilon) D'(\epsilon + \omega + l\hbar\omega_0) \\
&\times [n_{\mathrm{F}}(\epsilon) - n_{\mathrm{F}}(\epsilon + \omega + l\hbar\omega_0)] \Bigg\}.
\end{aligned}
$$

Here D' is the derivative of the density of states (which is zero for a constant DOS). In the figure for the optical conductivity, figure 6, we see that there is a large coherent Drude peak at low frequency, which disappears as the temperature increases, consistent with experiments done on the manganites [3]. The disappearance of the Drude peak is consistent with the peak in the spectral function disappearing; see figure 3. Such a behaviour has been observed [39] for Sr_2RuO_4, where the Drude peak disappeared above 100 K. Another system is $La_{0.825}Sr_{0.175}MnO_4$, where the Drude peak disappears above 200 K [40].

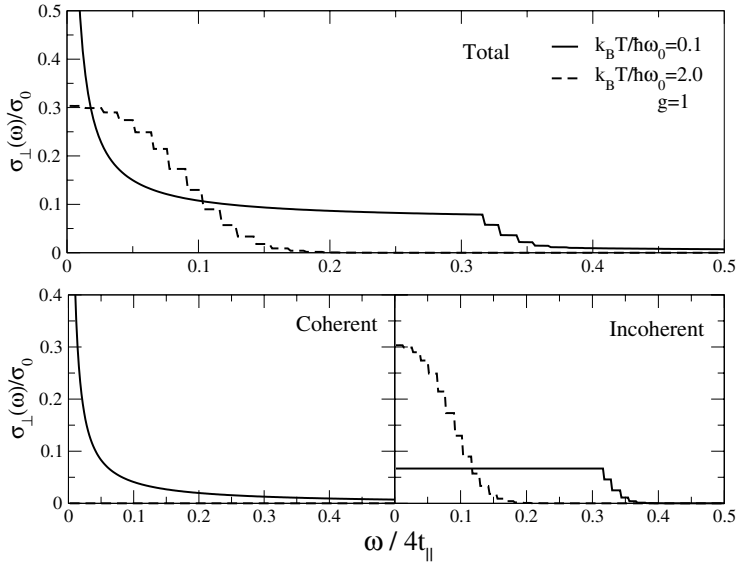

Figure 6. The top panel shows the frequency dependence of the interlayer optical conductivity for two different temperatures. The Drude peak (at $\omega = 0$) disappears when coherence is lost, due to the destruction of coherent quasi-particles with increasing temperature. The two lower panels show the optical conductivity divided into the two contributions, coherent and incoherent, plotted for two different temperatures. The input density of states is flat with a bandwidth of $W = 77\hbar\omega_0$.

4.5. Interlayer magnetoresistance for a field parallel to the layers

We can also make a statement about the magnetoresistance in a certain limit. If we apply a magnetic field, B, parallel to the layers (the x–y plane) there is an orbital effect on the paths of the electrons. This can be described as a shift in wavevector, $\mathbf{k} \to \mathbf{k} - \frac{e}{\hbar}\mathbf{A}$, where $\mathbf{A}$ is the vector potential for the magnetic field. For a magnetic field in the x direction, when an electron tunnels between adjacent layers it undergoes a shift in the y component of its wavevector by $-\mathrm{d}B$ [35]. In the general expression, equation (34), $|A(\mathbf{k}, \epsilon)|^2$ is replaced with an equation containing $A_1(\mathbf{k}, \epsilon)A_2(\mathbf{k} + \frac{e}{\hbar}\,\mathrm{d}B\vec{y})$, since there will be a difference in vector potential between the two layers.

However, since the incoherent part of the conductivity contains a summation over $\mathbf{k}$ space and is *independent* of $\mathbf{k}$, this will be unaffected by the magnetic field, i.e. $\sum_{\mathbf{p}} A_2^0(\mathbf{p} + \frac{e}{\hbar}\,\mathrm{d}B\vec{y}, \epsilon + eV) = \sum_{\mathbf{p}} A_2^0(\mathbf{p}, \epsilon + eV)$, since the sum spans over the first Brillouin zone.

Thus, we will have two contributions to the interlayer conductivity and one is B independent:

$$\sigma_\perp(B) = \sigma_\perp^{\mathrm{coh}}(B) + \sigma_\perp^{\mathrm{incoh}}(B = 0). \tag{43}$$

$\sigma^{\mathrm{coh}}(B)$ decreases with increasing magnetic field [41, 35]:

$$\sigma_\perp^{\mathrm{coh}}(B) = \frac{\sigma_\perp^{\mathrm{coh}}(B = 0)}{\sqrt{1 + (ev_{\mathrm{F}}\,\mathrm{d}B/\Gamma)^2}} \tag{44}$$

where v_{F} is the Fermi velocity. If we increase B, the coherent part decreases and, therefore, $T_\perp^{\max}$ will shift to *lower* values. A separation of the conductivity into two parts, as in equation (43), has been proposed previously [2] on a phenomenological basis, in order to describe the magnetoresistance of Sr_2RuO_4 (except that there a weak field dependence is associated with the incoherent contribution due to Zeeman splitting).

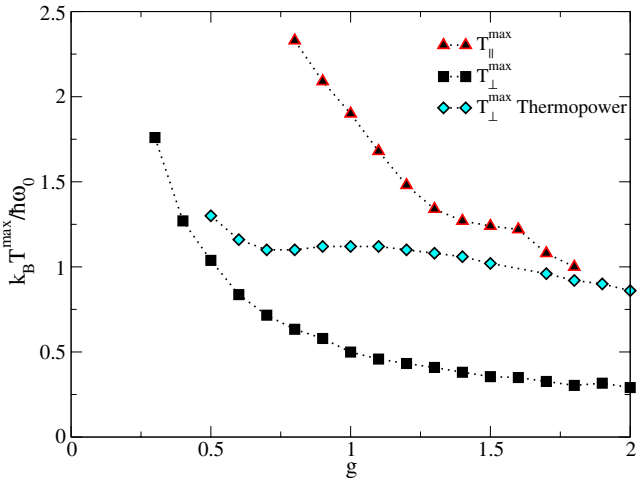

Figure 7. Crossover temperatures as a function of electron–phonon coupling constant, for the intralayer and interlayer resistivity, and the interlayer thermopower; for a fixed coupling and increasing temperature, first the coherence between the layers is lost, then there is a crossover peak in the interlayer thermopower and lastly the coherence within each layer is lost at elevated temperatures. The sequence of crossovers does not change if $t_{\parallel}/W$ is changed.

5. Discussion

We have presented a layered polaron model for systems consisting of two-dimensional layers coupled by tunnelling. We have found that when the temperature is lower than the characteristic boson frequency the physics is dominated by coherent transport where the electrons scatters off bosons in the layers. Upon increasing the temperature a transition is made into a region where the physics is governed by incoherent small polarons. The small polarons are localized at the lattice sites and hop to new sites. We have extracted results for intralayer and interlayer transport, thermopower, ARPES, optical conductivity and magnetoresistance.

In figure 7 we plot the different crossover temperatures as a function of the dimensionless electron–boson coupling.

The theory presented differs in the way polarons are formed from the theory by Ho and Schofield [42]. In their model the polarons are formed by a distortion of the interlayer distance to bind the polarons in a layer. We believe that this effect, although present, should be small due to the huge deformation energy involved. Their model does show the crossover from coherent to incoherent transport present in all polaron theories.

Acknowledgments

U Lundin acknowledges support from the Swedish foundation for international cooperation in research and higher education (STINT). This work was also supported by the Australian Research Council (ARC).

Appendix. The Green function in the high temperature limit

In order to calculate the intralayer conductivity at high temperatures, when polarons are formed and are localized, we need the GF. We perform perturbation theory in t and include the diagrams shown in figure A.1. When summing the series shown in figure A.1, we have to consider the

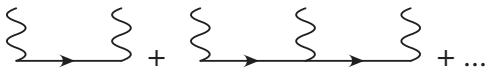

Figure A.1. The diagrams taken into account when calculating the self-energy for the trapped polaron in the high temperature limit.

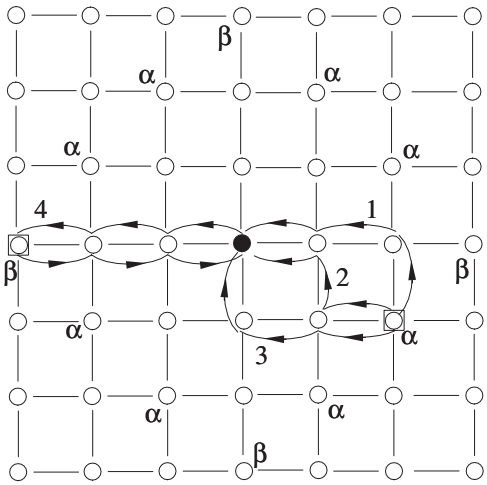

Figure A.2. An example when the polaron can hop three steps away, from the solid circle to the site marked with a box. From the sites marked with α there are three paths back (marked 1–3) and there are three paths there; there are eight such equivalent α sites. The polaron can also take the path to the site marked β; there are four equivalent sites of this type.

lattice that the electron moves in, i.e. the number of possible ways to return to the original site. In figure A.2 we have shown the number of possible paths when the polaron hops three jumps away from its original site. We have to find a general expression for the number of possible jumps for the whole lattice, and take into account identical paths.

Generally if the electron hops $2n$ steps, the number of possible paths is $4 + 2 \cdot 4n(n-1)$. Thus we get that the self-energy is

$$\Sigma(\omega, \Gamma) = 4 \sum_{n=1}^{\infty} [1 + 2n(n-1)] t^{2n} G^{2n-1} = 4t^2 G \frac{1 + t^2 G^2 + t^4 G^4}{(1 - t^2 G^2)^3}, \qquad \text{(A.1)}$$

where G is the local polaron GF and t is the hopping integral within the layer.

References

[1] Kimura T, Tomioka Y, Kuwahara H, Asamitsu A, Tamura M and Tokura Y 1996 *Science* **274** 1698
[2] Hussey N E, Mackenzie A P, Cooper J R, Maeno Y, Nishizaki S and Fujita T 1998 *Phys. Rev.* B **57** 5505
[3] Takenaka K, Sawaki Y and Sugai S 1999 *Phys. Rev.* B **274** 1698
[4] Valla T, Johnson P D, Yusof Z, Wells B, Li Q, Loureiro S M, Cava R J, Mikami M, Mori Y, Yoshimura M and Sasaki T 2002 *Nature* **417** 627
[5] Vozmediano M A H, López-Sancho M P and Guinea F 2003 *Phys. Rev.* B **68** 195122
[6] Lavrov A N, Kameneva M Yu and Kozeeva L P 1998 *Phys. Rev. Lett.* **81** 5636
[7] Mihály G, Kézsmárki I, Zámborszky F and Forró L 2000 *Phys. Rev. Lett.* **84** 2670
[8] Buravov L I, Kushch N D, Merzhanov V A, Osherov M V, Khomenko A G and Yagubskii E B 1992 *J. Physique* I **2** 1257
[9] Merino J and McKenzie R H 2000 *Phys. Rev.* B **61** 7996

[10] Alexandrov A S and Bratkovsky A M 1999 *J. Phys.: Condens. Matter* **11** 1989
[11] Salamon M B and Jaime M 2001 *Rev. Mod. Phys.* **73** 583
[12] Palstra T T M, Ramirez A P, Cheong S-W, Zegarski B R, Schiffer P and Zaanen J 1997 *Phys. Rev.* B **56** 5104
[13] Liu C-J, Sheu C-S and Huang M-S 2000 *Phys. Rev.* B **61** 14323
[14] Chen X J, Zhang C L, Almasan C C, Gardner J S and Sarrao J L 2003 *Phys. Rev.* B **67** 94426
[15] Billinge S J L, DiFrancesco R G, Kwei G H, Neumeier J J and Thompson J D 1996 *Phys. Rev. Lett.* **77** 715
[16] Adams C P, Lynn J W, Mukovskii Y M, Arsenov A A and Shulyatev D A 2000 *Phys. Rev. Lett.* **85** 3954
[17] Campbell B J, Sinha S K, Osborn R, Rosenkranz S, Mitchell J F, Argyriou D N, Vasiliu-Doloc L, Seeck O H and Lynn J W 2003 *Science* **67** 020409
[18] Choi E S, Brooks J S and Qualls J S 2002 *Phys. Rev.* B **65** 205119
[19] Mannella N, Rosenhahn A, Booth C H, Marchesini S, Mun B S, Yang S-H, Ibrahim K, Tomioka Y and Fadley C S 2004 *Phys. Rev. Lett.* **92** 166401
[20] Mahan G D 1990 *Many-Particle Physics* 2nd edn (New York: Plenum)
[21] Appel J 1968 *Solid State Physics* vol 21 (New York: Academic)
[22] Fratini S and Ciuchi S 2003 *Phys. Rev. Lett.* **91** 256403
[23] Liu X, Zhu H and Zhang Y 1996 *Phys. Rev.* B **65** 024412
[24] Alexandrov A S and Bratkovsky A M 1999 *Phys. Rev. Lett.* **82** 141
[25] Alexandrov A S, Zhao G, Keller H, Lorenz B, Wang Y S and Chu C W 2001 *Phys. Rev.* B **64** 140404
[26] Weisse A, Loos J and Fehske H 2003 *Phys. Rev.* B **68** 024402
[27] Lundin U and McKenzie R H 2003 *Phys. Rev.* B **68** 081101
[28] Lundin U and McKenzie R H 2004 Magic angles in quasi-1D metals due to intralayer incoherence *Preprint* cond-mat/0404528
[29] Holstein T 1959 *Ann. Phys.* **8** 343
[30] Lang I G and Firsov Yu A 1963 *Sov. Phys. JETP* **16** 1301
[31] Alexandrov A S and Mott N 1995 *Polarons and Bipolarons* (Singapore: World Scientific)
[32] Karlsson E B 1998 *New Perspectives on Problems in Classical and Quantum Physics* (New York: Gordon and Breach)
[33] Ciuchi S, de Pasquale F, Fratini S and Feinberg D 1997 *Phys. Rev.* B **56** 4494
[34] Wang S C, Yang H B, Sekharan A K P, Ding H, Engelbrecht J R, Dai X, Wang Z, Kaminski A, Valla T, Kidd T, Fedorov A V and Johnson P D 2004 *Phys. Rev. Lett.* **92** 137002
[35] Moses P and McKenzie R H 1999 *Phys. Rev.* B **60** 7998
[36] Adler D 1968 *Solid State Physics* vol 21 (New York: Academic)
[37] Emin D 1975 *Phys. Rev. Lett.* **35** 882
[38] Jaime M, Salamon M B, Rubinstein M, Treece R E, Horowitz J S and Chrisey D B 1996 *Phys. Rev.* B **54** 11914
[39] Katsufuji T, Kasai M and Tokura Y 1996 *Phys. Rev. Lett.* **76** 126
[40] Takenaka K, Sawaki Y, Shiozaki R and Sugai S 2000 *Phys. Rev.* B **62** 13864
[41] Schofield A J and Cooper J R 2000 *Phys. Rev.* B **62** 10779
[42] Ho A F and Schofield A J 2002 Small polarons and *c*-axis transport in highly anisotropic metals *Preprint* cond-mat/0211675